

Shape coexistence in even–even Po isotopic chain

S. Shohani and A. Kardan*
*School of Physics, Damghan University,
Damghan, Iran*
*aakardan@du.ac.ir

Received 15 August 2019
Revised 27 October 2019
Accepted 27 October 2019
Published 3 December 2019

The Po isotopes show the presence of coexisting structures having different deformations with increasing neutron number within the macroscopic–microscopic Nilsson–Strutinsky formalism. The model is based on the Lublin Strasbourg Drop (LSD) method for the macroscopic energy calculation. We study the shape evolution in a long chain of polonium isotopes, $^{178-200}\text{Po}$.

Keywords: Shape coexistence; Nilsson–Strutinsky model; macroscopic LSD model; Po isotopes.

PACS Number(s): 21.60.n, 21.10.k

1. Introduction

One of the remarkable properties of the nuclear quantum many-body system is the ability to minimize energy by adopting different nuclear shapes with a relatively small cost in energy compared to the total binding energy.¹ It has been experimentally shown that the closed-shell nuclei have a spherical shape. In the case of a prolate shape, the lower half of nuclei shell is filled by nucleons while in an oblate one, the upper half is filled.² Now, the question is what happens if a shell is filled up to its middle. It is evident that different shapes may coexist with approximately similar energy values even at high spins.³

The shape coexistence phenomenon and understanding of its origin are an interesting subject and a challenging problem in the nuclear structure physics.⁴ Isotope shifts have played a very important role in the discovery of shape coexistence through the appearance of sudden changes that herald the intrusion of strongly deformed configurations to dominate ground state structures.⁵ However, coexisting minima are understood well in the context of the nuclear shell model as arising from

*Corresponding author.

intruder excitations particularly in the near closed-shell regions.⁶ The shape coexistence phenomenon in the $A \sim 190$ mass region has attracted many researchers over a number of years.^{7–11} There is some evidence on unusual features of some of their isotopic chains with an abrupt variation of particular nuclear properties. The shape coexistence has been observed, experimentally, in $^{180-190}\text{Hg}$,¹² $^{188-194}\text{Pb}$,⁹ and in some heavier Tl^{13} and Au^{14} isotopes. In the vicinity of $Z = 82$, the interplay between microscopic and macroscopic effects gives rise to shape coexistence at low energy.^{7–9} The extent of the mixing between the different shapes can be determined by investigating the evolution of the shape of the nucleus in its ground state through the study of the potential energy surfaces (PES).

In this work, we intend to study the shape evolution of even–even Po isotopic chain, where the shape coexistence phenomena are not clear enough. We carry out the calculations within the Nilsson–Strutinsky model, which is a macroscopic–microscopic method.^{15–17} A similar study has been performed recently in the $A \sim 80$ mass region.¹⁸

2. The Model

The total energy E_{tot} of a nucleus with a given deformation is calculated in the macroscopic–microscopic approach as

$$E_{\text{tot}} = E_{\text{macro}} + E_{\text{micro}}, \quad (1)$$

where each contribution depends on the deformation. The total energy is calculated at each deformation parameter (ε_2 , γ and ε_4).

The macroscopic part is calculated within the Lublin–Strasbourg drop (LSD) model¹⁹, which is a liquid-drop-type parametrization of the nuclear energy including a curvature term proportional to $A^{1/3}$. The LSD prescription has shown to yield a good description of both nuclear ground state masses and fission-barrier heights. The microscopic part consists of the proton and neutron shell corrections as

$$E_{\text{sh}} = E_{\text{sh}}(\text{protons}) + E_{\text{sh}}(\text{neutrons}). \quad (2)$$

For each kind of particle, shell corrections are obtained by subtracting the average energy from the sum of the single-particle energy of the occupied orbitals as

$$E_{\text{sh}} = \sum_k e_k - \widetilde{\sum_k e_k}. \quad (3)$$

The smooth energy $\widetilde{\sum_k e_k}$ is evaluated using the Strutinsky method.²⁰ In the present formalism, the single-particle Hamiltonian is the modified oscillator Nilsson potential. The PES is calculated by minimizing the total energy with respect to the hexadecapole parameters and plotting in the (ε_2, γ) plane. The standard parameter set¹⁵ is used for the Nilsson single-particle parameters κ and μ in the modified

harmonic oscillator (MHO) Hamiltonian.²¹

$$H_{\text{MHO}} = \frac{P^2}{2m} + \frac{1}{2}m(\omega_x^2 x^2 + \omega_y^2 y^2 + \omega_z^2 z^2) - \kappa \hbar \omega_0 [2\ell \cdot s + \mu(\ell_t - \langle \ell_t \rangle)] + V_4(\varepsilon_4, \gamma), \quad (4)$$

where $V_4(\varepsilon_4, \gamma)$ represents the hexadecapole deformation potential.¹⁷

3. Results and Discussions

The total energy of Po isotopes is obtained theoretically in the three-dimensional deformation space for about 1600 different nuclear shapes. The deformation energy landscape was calculated, in this study, according to the approach outlined in the previous section for 12 A -even polonium isotopes from ^{178}Po to ^{200}Po . Figure 1 illustrates the PES for the target isotopes for which the dark region represents the lowest energy. The interval between the contour lines is about 0.25 MeV and the γ -plane is marked at 15° intervals. If the minimum is observed at $\gamma = 0^\circ$ or -120° , the nucleus possesses a prolate shape; if $\gamma = 60^\circ$ or -60° , it will have an oblate shape. However, a dark region between these angles shows that the shape is approximated as a triaxial ellipsoid. Absolutely, the deformation parameter $\varepsilon_2 \sim 0$ represents a spherical shape. Moreover, semicircular dash lines determine the deformation parameter ε_2 .

As the polonium nucleus has the atomic number $Z = 84$ near a closed shell of $Z = 82$, it is expected that the protons create a near spherical shape. Consequently, the neutron number will have an effect on the nuclear shape in the Po isotopes. As seen in Fig. 1, the PES of ^{200}Po , with a neutron number $N = 116$, shows a sharp well with one minimum at a small deformation $\varepsilon_2 \sim 0.12$ with a small triaxiality. With decreasing two neutrons, not only a flat-well at $\varepsilon_2 \sim 0.12$ which is the yrast state in ^{198}Po , but also one local minimum appears at $\varepsilon_2 \sim 0.2$ with a higher energy about 750 keV than the energy of the yrast state.

In $^{196,194}\text{Po}$ isotopes, two separated local minima appear at $\varepsilon_2 \sim 0.2$. It is observed that these local minima become the yrast state in ^{192}Po isotope with two less neutrons. In $^{192-188}\text{Po}$, the prolate and oblate shapes coexist at deformation parameters $(\varepsilon_2, \gamma) \sim (0.1, -120^\circ)$ and $(0.25, -60^\circ)$, respectively. As a result, by decreasing the neutron number, it appears more minima in the PES of $^{186-182}\text{Po}$ at various shapes including prolate, oblate, spherical and triaxial shapes. It even demonstrates the prolate and oblate minima at larger deformations $\varepsilon_2 \sim 0.3$ and 0.4 , respectively, in which the later one is more clear in ^{184}Po . These various shapes in the PES are also observed in some lead isotopes; for example, see Fig. 1 in Refs. 22 and 23. If the neutron number still decreases, the minima will drop to one minimum at the prolate shape with $\varepsilon_2 \sim 0.16$ leading to the disappearing of the shape coexistence in $^{180,178}\text{Po}$.

Accordingly, to be $N = 104$ at the middle of the shell gaps $N = 82$ and 126 , it is concluded to observe the shape coexistence in ^{188}Po and its neighboring isotopes.

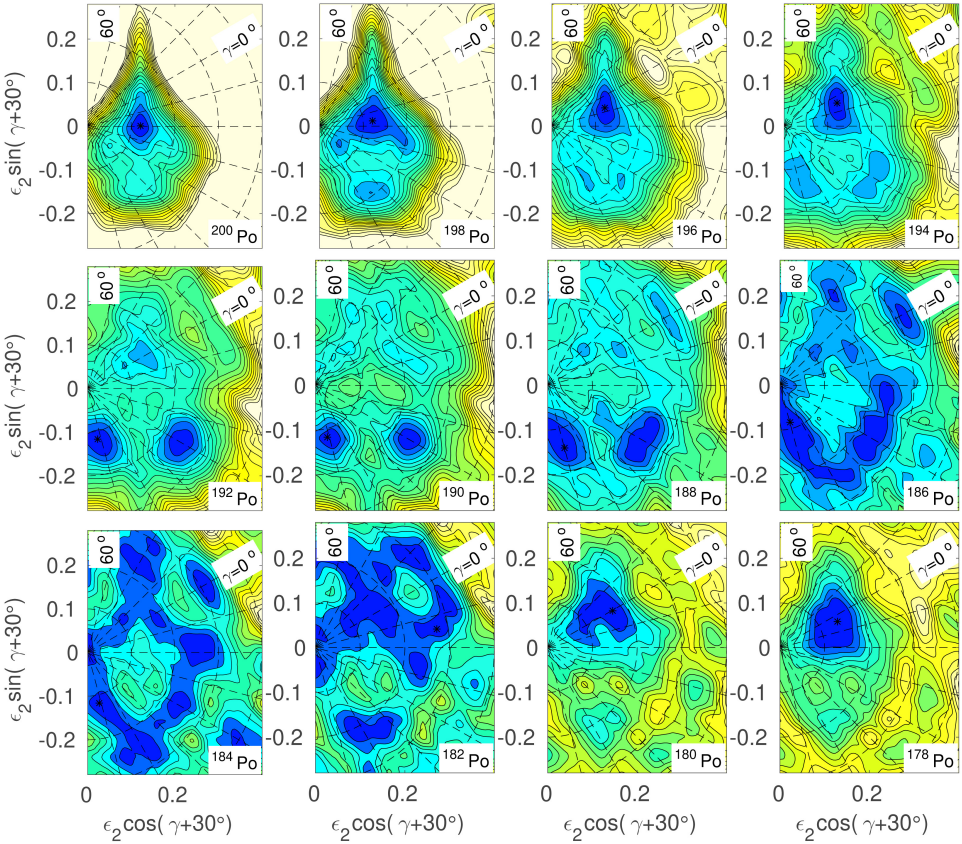


Fig. 1. Potential energy surfaces of the Po isotopes ($Z = 84$) from neutron number $N = 94$ to 116 in the (ϵ_2, γ) plane and at the ground state, obtained from the Nilsson–Strutinsky calculations. The contour line separation is 0.25 MeV.

This observation is consistent with our results where the shape coexistence is seen in Fig. 1 for $^{182-192}\text{Po}$ isotopes which ^{188}Po is the center of this region. The observed rotational bands based on both oblate²⁴ and prolate²⁵ shapes in $^{186,188}\text{Pb}$ confirm the current evidence. We also expect to reach an oblate shape when the upper half of the neutron shell is filling while a prolate shape appears when the lower half of the neutron shell is filling. The PES diagrams of Fig. 1 are in good agreement with these expectations. For heavier isotopes $^{194-200}\text{Po}$ where the neutron orbitals p and $i_{13/2}$ are filling, the minimum inclines to appear at the oblate deformation with a triaxiality degree so that the γ value increases at greater neutron numbers. While a prolate shape for the lighter isotopes $^{178-180}\text{Po}$ is observed where the neutron orbitals hf start to be occupied.

More complicated PESs may be seen in the polonium isotopes compared with the situation in the lead isotopes.²⁶ Configuration-constrained PES calculations

have been performed to investigate the shape coexistence phenomenon in neutron-deficient polonium isotopes.²⁶ As a consequence, the shape coexistence phenomenon is observed in the isotopes $^{190-194}\text{Po}$, see Fig. 3 in Ref. 26, which matches well with the present calculations. A comparatively flat prolate minima for $^{196,198}\text{Po}$ are found which is compatible with the Nilsson–Strutinsky method results. Our calculations also display oblate minima at $\varepsilon_2 \sim -0.25$ and prolate minima at $\varepsilon_2 \sim 0.15$, which is different with the results of Ref. 26 where the oblate and prolate minima are at $\varepsilon_2 \sim -0.19$ and 0.24 , respectively.

Therefore, one can conclude from the present calculations that the shape coexistence phenomenon is clearly observed in $^{182-192}\text{Po}$ isotopes with various shapes of the spherical, prolate, oblate and triaxial.

4. Summary

Investigation of shape coexisting ground state in polonium isotopes was carried out by using the macroscopic–microscopic Nilsson–Strutinsky model. We presented the results for shape phase transitions in the chain of Po isotopes from $A = 178$ to 200. It is found that the considered polonium isotopes present a clear example of the coexistence of spherical, oblate and prolate equilibrium shapes such as in its neighboring nuclei, Hg and Pb.^{2,9,12} The PES curves for Po isotopes (Fig. 1) exhibit a complicated coexistence of several shallow minima specially for the isotopes $^{182-186}\text{Po}$. The calculations show a clear shape coexistence in the isotopes $^{182-192}\text{Po}$.

The shape coexistence and shape transition are associated with the occupation of some specific single-particle structure. In Po isotopes, the occupation of the neutron intruder state $i_{13/2}$ gives rise to the prolate shape and shape coexistence. The present findings are in general similar to the obtained results by Skyrme-HFB²⁷ and also configuration-constrained PES calculations²⁶ on the shape coexistence in Po isotopes.

References

1. R. Wadsworth *et al.*, *Phys. Lett. B* **701** (2011) 306.
2. C. F. Jiao, Y. Shi, H. L. Liu, F. R. Xu and P. M. Walker, *Phys. Rev. C* **91** (2015) 034309.
3. P. M. Walker, F. R. Xu and D. M. Cullen, *Phys. Rev. C* **71** (2005) 067303.
4. J. L. Wood and K. Heyde, *Rev. Mod. Phys.* **83** (2011) 1467.
5. J. L. Wood and K. Heyde, *J. Phys. G Nucl. Part. Phys.* **43** (2016) 020402.
6. A. Frank, P. V. Isacker and C. E. Vargas, *Phys. Rev. C* **69** (2004) 034323.
7. J. L. Wood, K. Heyde, W. Nazarewicz, M. Huyse and P. Van Duppen, *Phys. Rep.* **215** (1992) 101.
8. K. Heyde, P. Van Isacker, M. Waroquier, J. L. Wood and R. A. Meyer, *Phys. Rep.* **102** (1983) 291.
9. R. Julin, K. Helariutta and M. Muikku, *J. Phys. G Nucl. Part. Phys.* **27** (2001) R109.
10. M. D. Seliverstov *et al.*, *Phys. Rev. C* **89** (2014) 034323.
11. A. Rohilla *et al.*, *Eur. Phys. J. A* **53** (2017) 64.

12. F. Hannachi *et al.*, *Nucl. Phys. A* **481** (1988) 135.
13. W. Reviol *et al.*, *Phys. Rev. C* **58** (1998) R2644.
14. D. Rupnik *et al.*, *Phys. Rev. C* **58** (1998) 771.
15. T. Bengtsson and I. Ragnarsson, *Nucl. Phys. A* **436** (1985) 14.
16. B. G. Carlsson and I. Ragnarsson, *Phys. Rev. C* **74** (2006) 011302(R).
17. A. Kardan, I. Ragnarsson, H. Miri-Hakimabad and L. Rafat-Motevali, *Phys. Rev. C* **86** (2012) 014309.
18. M. Akbari and A. Kardan, *Nucl. Phys. A* **990** (2019) 109.
19. K. Pomorski and J. Dudek, *Phys. Rev. C* **67** (2003) 044316.
20. V. M. Strutinsky, *Nucl. Phys. A* **122** (1968) 1.
21. A. Kardan and S. Sayyah, *Int. J. Mod. Phys. E* **25** (2016) 1650044.
22. T. Duguet, M. Bender, P. Bonche and P.-H. Heenen, *Phys. Lett. B* **559** (2003) 201.
23. R. R. Rodriguez-Guzmn, J. L. Egido and L. M. Robledo, *Phys. Rev. C* **69** (2004) 054319.
24. J. Pakarinen *et al.*, *Phys. Rev. C* **75** (2007) 014302.
25. W. Reviol, C. J. Chiara, O. Pechenaya, D. G. Sarantites, P. Fallon and A. O. Macchiavelli, *Phys. Rev. C* **75** (2003) 014302.
26. Y. Shi, F. R. Xu, H. L. Liu and P. M. Walker, *Phys. Rev. C* **82** (2010) 044314.
27. N. A. Smirnova, P.-H. Heenen and G. Neyens, *Phys. Lett. B* **569** (2003) 151.